Computer Applications in Electrical Engineering
Vol. 12 *2014*

Current density in the unscreened three-phase high-current busduct

Tomasz Szczegielniak, Zygmunt Piątek, Dariusz Kusiak
Częstochowa University of Technology
42-200 Częstochowa, ul. Brzeźnicka 60a
e-mail: zygmunt.piatek@interia.pl, dariuszkusiak@wp.pl,
szczegielniakt@interia.pl

Design of the high-current busducts on high currents and voltages causes necessity precise describing of electromagnetic, dynamic and thermal effects. Knowledge of the relations between electrodynamics and constructional parameters is necessary in the optimization construction process of the high-current busducts. Information about distribution electromagnetic field is a base into analysis of electrodynamics and thermal effects in the high-current busducts. The paper presents analytical calculations of the current density in the three-phase high-current busduct which phase conductors are placed in vertex of a square. Into account were taken skin and proximity effect. The electromagnetic field produced by high-current busducts are usually calculated numerically with the use of a computer. However, the analytical calculation of the electromagnetic field is preferable, because it results in a mathematical expression for showing its dependences on various parameters of the line arrangement.

KEYWORDS: analytical method, high-current busduct, current density

1. Introduction

Busbar systems are today widely employed in the industrial environment for electrical energy distribution. The main advantages of these devices are linked to their modularity that enables fast and easy installation, plant modification, and maintenance [1-9]. Several manufacturers in the market propose busbar systems form few to thousand amperes. Their design seems to be quite easy and for a long time, thanks to the experimental knowledge, different types and size have been designed using scalar rules. The bus ducts usually consist of aluminum or copper busbars [1-9]. A typical shielded three-phase high-current busduct is depicted in Figure 1.

The design of the busducts used for high currents and voltages requires the precise analysis of electromagnetic, dynamic and thermal effects. Knowledge of the relations between electrodynamics and constructional parameters is necessary in the optimization construction process of the high-current busducts [1-9].

Fig. 1. 245 kV GIL Cairo North [9]

Electromagnetic field depends on value of currents, and for the large cross-sectional dimensions of the phase conductor, even at industrial frequency, skin and proximity effect (Fig. 2) should be taken into account [1-8].

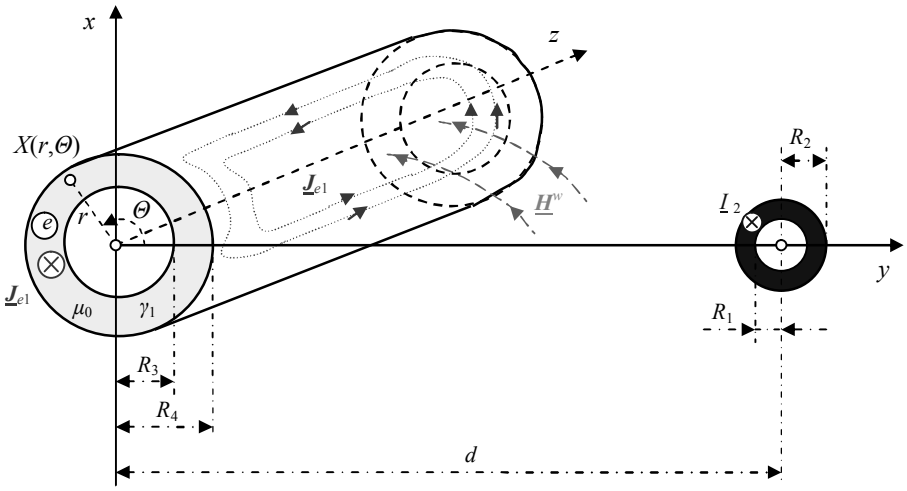

Fig. 2. Eddy currents induced in the screen by the magnetic field of the neighboring phase conductor

2. Current density

The most popular solution of the high-current busducts are symmetrical or flat [2-8]. In this paper the analytical calculations of the current density in the high-current busduct which phase conductors are placed in vertex of a square will be presented (Fig. 3).

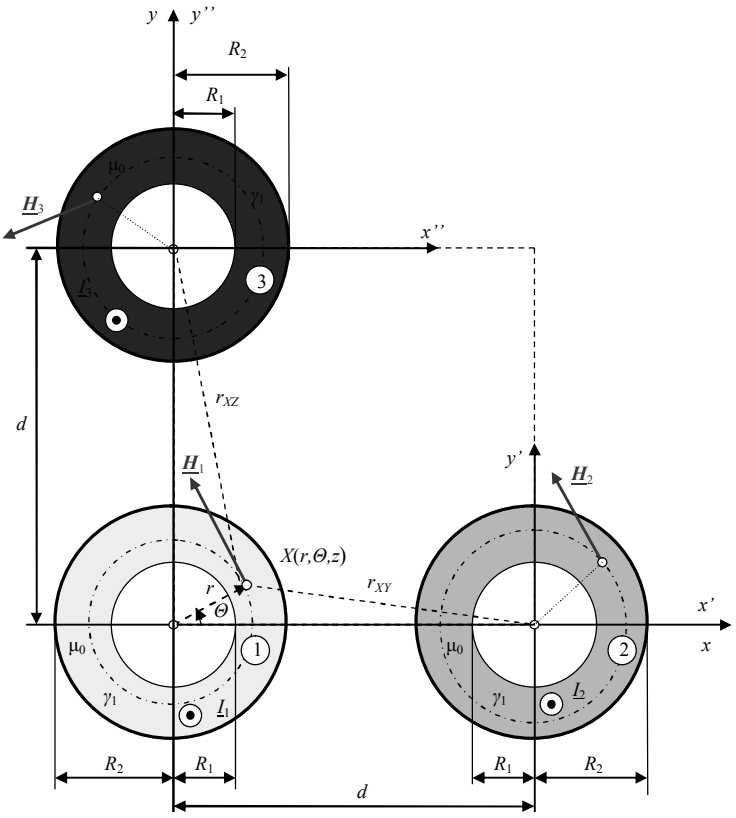

Fig. 3. Three-phase high-current busduct which phase conductors are placed in vertex of a square

Let us consider the electromagnetic field in a three-pole high-current busduct presented in the fig. 3. Using the Laplace's and Helmoltz's equations we can determine the electromagnetic field in the conductors. The total current density in the first conductor is a sum of currents induced by each conductor, that is to say

$$\underline{\boldsymbol{J}}_1(r,\Theta) = \underline{\boldsymbol{J}}_{11}(r) + \underline{\boldsymbol{J}}_{12}(r,\Theta) + \underline{\boldsymbol{J}}_{13}(r,\Theta) = \mathbf{1}_z\left[\underline{J}_{11}(r) + \underline{J}_{123}(r,\Theta)\right] = \mathbf{1}_z\,\underline{J}_1(r,\Theta) \quad (1)$$

where

$$\underline{J}_{11}(r)=\frac{\underline{\Gamma}\,\underline{I}_1}{2\pi R_2}\frac{K_1(\underline{\Gamma}R_1)I_0(\underline{\Gamma}r)+I_1(\underline{\Gamma}R_1)K_0(\underline{\Gamma}r)}{I_1(\underline{\Gamma}R_2)K_1(\underline{\Gamma}R_1)-I_1(\underline{\Gamma}R_1)K_1(\underline{\Gamma}R_2)}=\frac{\underline{\Gamma}\,\underline{I}_1}{2\pi R_2}\underline{j}(r) \tag{2}$$

and

$$\underline{J}_{12}(r,\Theta)=-\frac{\underline{\Gamma}\,\underline{I}_2}{\pi R_2}\sum_{n=1}^{\infty}\left(\frac{R_2}{d}\right)^n \underline{f}_n(r)\cos n\Theta = J_{12}(r,\Theta)\exp[\mathrm{j}\varphi_{J12}(r,\Theta)] \tag{3}$$

$$\underline{f}_n(r)=\frac{K_{n+1}(\underline{\Gamma}R_1)I_n(\underline{\Gamma}r)+I_{n+1}(\underline{\Gamma}R_1)K_n(\underline{\Gamma}r)}{I_{n-1}(\underline{\Gamma}R_2)K_{n+1}(\underline{\Gamma}R_1)-I_{n+1}(\underline{\Gamma}R_1)K_{n-1}(\underline{\Gamma}R_2)} \tag{3a}$$

$$\underline{J}_{13}(r,\Theta)=-\frac{\underline{\Gamma}\,\underline{I}_3}{\pi R_2}\sum_{n=1}^{\infty}\left(\frac{R_2}{d}\right)^n \underline{f}_n(r)\cos n\left(\Theta-\frac{\pi}{2}\right) \tag{4}$$

For the positive sequence of currents, i.e.

$$\underline{I}_2=\exp[-\mathrm{j}\frac{2}{3}\pi]\,\underline{I}_1 \quad \text{and} \quad \underline{I}_3=\exp[\mathrm{j}\frac{2}{3}\pi]\,\underline{I}_1 \tag{5}$$

the total current density in first conductor has the following form

$$\underline{J}_1(r,\Theta)=\underline{J}_{11}(r)+\underline{J}_{123}(r,\Theta)=\frac{\underline{\Gamma}\,\underline{I}_1}{2\pi R_2}\left[\underline{j}(r)-2\sum_{n=1}^{\infty}\underline{A}_n\left(\frac{R_2}{d}\right)^n \underline{f}_n(r)\right] \tag{6}$$

where

$$\underline{A}_n=\exp\left[-\mathrm{j}\frac{2}{3}\pi\right]\cos n\Theta+\exp\left[\mathrm{j}\frac{2}{3}\pi\right]\cos n\left[\Theta-\frac{\pi}{2}\right] \tag{6a}$$

The total current density in the second conductor is described by

$$\underline{\boldsymbol{J}}_2(r,\Theta)=\underline{\boldsymbol{J}}_{22}(r)+\underline{\boldsymbol{J}}_{21}(r,\Theta)+\underline{\boldsymbol{J}}_{23}(r,\Theta)=\mathbf{1}_z\left[\underline{J}_{22}(r)+\underline{J}_{213}(r,\Theta)\right]=\mathbf{1}_z\,\underline{J}_2(r,\Theta) \tag{7}$$

in which current density $\underline{J}_{22}(r)$ are described by Eq. (2) in which current $\underline{I}_1$ should be replaced with $\underline{I}_2$, but current density

$$\underline{J}_{213}(r,\Theta)=-\frac{\underline{\Gamma}\,\underline{I}_2}{\pi R_2}\sum_{n=1}^{\infty}\underline{B}_n(-1)^n\left(\frac{R_2}{d}\right)^n \underline{f}_n(r) \tag{8}$$

where

$$\underline{B}_n=\exp\left[\mathrm{j}\frac{2}{3}\pi\right]\cos n\Theta+\left(\frac{1}{\sqrt{2}}\right)^n\exp\left[-\mathrm{j}\frac{2}{3}\pi\right]\cos n\left[\Theta+\frac{\pi}{4}\right] \tag{8a}$$

For the third conductor, the total current density is

$$\underline{\boldsymbol{J}}_3(r,\Theta)=\underline{\boldsymbol{J}}_{33}(r)+\underline{\boldsymbol{J}}_{31}(r,\Theta)+\underline{\boldsymbol{J}}_{32}(r,\Theta)=\mathbf{1}_z\left[\underline{J}_{33}(r)+\underline{J}_{312}(r,\Theta)\right]=\mathbf{1}_z\,\underline{J}_3(r,\Theta) \tag{9}$$

in which current density $\underline{J}_{33}(r)$ are described by Eq. (2) in which current $\underline{I}_1$ should be replaced with $\underline{I}_3$, and current density

$$\underline{J}_{312}(r,\Theta) = -\frac{\underline{\Gamma}\,\underline{I}_3}{\pi R_2}\sum_{n=1}^{\infty}\underline{C}_n\left(\frac{R_2}{d}\right)^n \underline{f}_n(r) \tag{10}$$

where

$$\underline{C}_n = (-1)^n \exp\left[-\mathrm{j}\frac{2}{3}\pi\right]\cos n\left[\Theta - \frac{\pi}{2}\right] + \left(\frac{1}{\sqrt{2}}\right)^n \exp\left[\mathrm{j}\frac{2}{3}\pi\right]\cos n\left[\Theta + \frac{\pi}{4}\right] \tag{10a}$$

In the above formulas $I_0(\underline{\Gamma}r)$, $K_0(\underline{\Gamma}r)$, $I_1(\underline{\Gamma}r)$, $K_1(\underline{\Gamma}r)$, $I_n(\underline{\Gamma}r)$, $K_n(\underline{\Gamma}r)$, $I_{n-1}(\underline{\Gamma}r)$, $K_{n-1}(\underline{\Gamma}r)$, $I_{n+1}(\underline{\Gamma}r)$ and $K_{n+1}(\underline{\Gamma}r)$ are the modified Bessel's functions of order 0, 1, n, n-1 and n+1, calculated for $r = R_1$ and $r = R_2$ [10], and the complex propagation constant of electromagnetic wave in the conductor equals

$$\underline{\Gamma} = \sqrt{\mathrm{j}\omega\mu_0\gamma} = \sqrt{\omega\mu_0\gamma}\,\exp[\mathrm{j}\frac{\pi}{4}] = k + \mathrm{j}\,k = \sqrt{2\mathrm{j}}\,k \tag{11}$$

with the attenuation constant

$$k = \sqrt{\frac{\omega\mu_0\gamma}{2}} = \frac{1}{\delta} \tag{12}$$

where δ is the electrical skin depth of the electromagnetic wave penetration into the conducting environment, ω is the angular frequency, γ stands for the conductivity of conductor, and $\mu_0 = 4\pi\,10^{-7}\ \mathrm{H\cdot m^{-1}}$ is the magnetic permeability of the vacuum.

If we introduce the parameters: $\beta = \frac{R_1}{R_2}$, $(0 \le \beta \le 1)$, $\lambda = \frac{d}{R_2} \ge 1$, $\alpha = \frac{R_2}{\delta} = k\,R_2$, $\xi = \frac{r}{R_2}$, $(\beta \le \xi \le 1)$ and the reference current density

$$\underline{J}_0 = \frac{\underline{I}_1}{\pi\left(R_2^2 - R_1^2\right)} \tag{13}$$

then the relative current density in the first conductor has a form

$$k_1 = \frac{\underline{J}_1}{\underline{J}_0} \tag{14}$$

In the same way we can calculate the relative current density in the second and third conductor. Dependence of the relative current densities on parameter α for different values of the relative walls thickness β and of relative distance between conductors λ is presented in the Fig. 4.

An analytical method presented in the paper can be used only for circular high-current busducts. Current density in the high-current busducts can be determined by specified computer program (for example FEMM, Fig. 5. [11]). However, the analytical calculation of the electromagnetic field is preferable,

because it results in a mathematical expression for showing its dependences on various parameters of the line arrangement.

a)

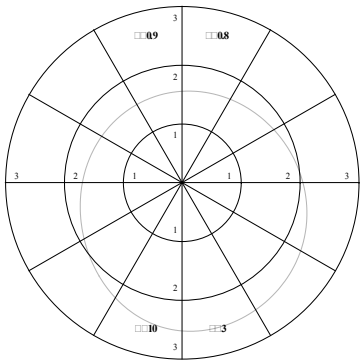

b)

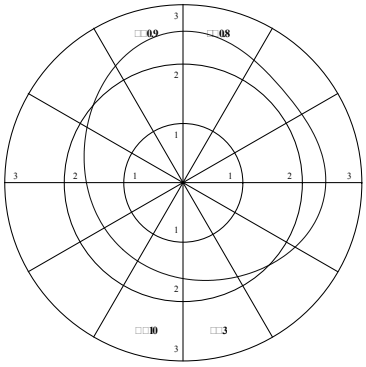

c)

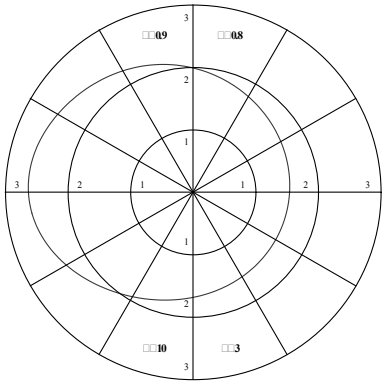

Fig. 4. Relative current density: a) in the third conductor, b) in the first conductor, c) in the second conductor

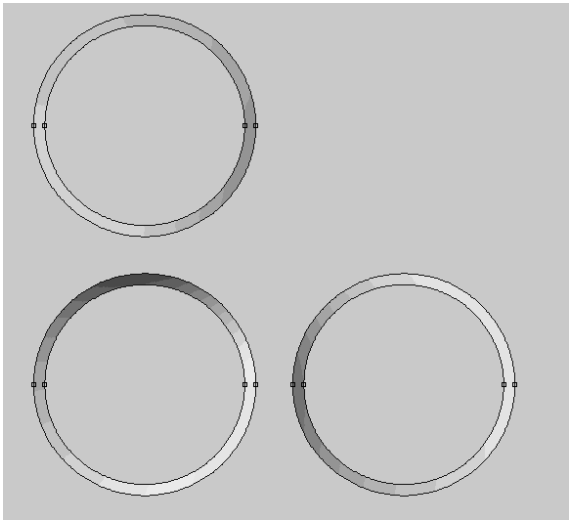

Fig. 5. Magnitude of current density in the high-current busduct which phase conductors are placed in vertex of a square

3. Conclusions

The paper presents an analytical method for determining the current density in the three-phase high-current busduct of circular cross-section geometry. The mathematical model takes into account the skin effect and the proximity effects. The current density occurs in the high-current busducts are usually calculated numerically with the use of a computer. However, the analytical calculation of the electromagnetic field is preferable, because it results in a mathematical expression for showing its dependences on various parameters of the line arrangement. Moreover, knowledge of the relations between electrodynamics and constructional parameters is necessary in the optimization construction process of the high-current busducts.

Presented in the figure 3 system of tubular conductors is the most often installed when symmetrical or flat high-current busduct can not be used. This situation appears in the narrow tunnels, shafts, cable ducts.

References

[1] Nawrowski R.: Tory wielkoprądowe izolowane powietrzem lub SF_6. Wyd. Pol. Poznańskiej, Poznań 1998.

[2] Piątek Z.: Impedances of high-current busducts. Wyd. Pol. Częst., Czestochowa 2008.

[3] Szczegielniak T.: Straty mocy w nieekranowanych i ekranowanych rurowych torach wielkoprądowych, Praca Doktorska, Gliwice, 2011.

[4] Piątek Z., Szczegielniak T., Kusiak D.: Straty mocy w płaskim rurowym trójfazowym torze wielkoprądowym, Wiadomości Elektrotechniczne, nr 11, s. 9-13, 2009.
[5] Piątek Z., Kusiak D., Szczegielniak T.: Pole magnetyczne oddziaływania zwrotnego w dwuprzewodowym nieekranowanym torze wielkoprądowym, XV Conference Computer Applications in Electrical Engineering, Poznań 2010, ss. 33-34.
[6] Piątek Z ., Szczegielniak T., Kusiak D.: Wpływ zewnętrznego zjawiska zbliżenia na straty mocy w trójfazowym płaskim torze wielkoprądowym, XVI Conference Computer Applications in Electrical Engineering, s 15-16 Poznań 2011.
[7] Kusiak D., Piątek Z., Szczegielniak T.: The Asymmetry of the Magnetic Field Distribution in a Flat Unshielded 3-Phase High Current Busduct, Acta Technica Jaurinensis Vol.6 nr 1, s.49-55, 2013.
[8] Szczegielniak T., Piątek Z ., Kusiak D.: Analiza gęstości prądów w nieosłoniętym trójfazowym torze wielkoprądowym, Computer Applications in Electrical Engineering, s 79-84, Poznań 2014.
[9] Koch H.: Gas-Insulated Transmission Lines, John Wiley&Sons, Ltd. 2012.
[10] Mc Lachlan N.W.: Funkcje Bessela dla inżynierów. PWN, Warszawa 1964.
[11] MEEKER, D.C.: Finite Element Method Magnetics, version 4.2 (11apr2012, Mathematica Build), http://www.femm.info.